

Upper Bound Analysis of Deformation and Dynamic Ageing Behavior in Elevated Temperature Equal Channel Angular Pressing of Al-Mg-Si Alloys

Majid Vaseghi^{1,2}, Ali Karimi Taheri^{1,*} and Hyoung Seop Kim²

¹ Department of Materials Science and Engineering,
Sharif University of Technology,
Tehran, 11155-9466, Iran

² Department of Materials Science and Engineering,
Pohang University of Science and Technology,
Pohang-si, Gyeongbuk 790-784, Korea

(received date: 17 June 2009 / accepted date: 10 September 2009)

In the present study, the plastic deformation and dynamic strain ageing behavior of Al-6082 (Al-Mg-Si) alloy treated with elevated temperature equal channel angular pressing (ECAP) were investigated using upper bound analyses. Tensile tests were carried out over wide ranges of temperature and strain rate in order to evaluate the dynamic ageing conditions. ECAP processing was then experimentally performed at temperatures from room temperature up to 200 °C under various strain rates ranging between 10^{-4}s^{-1} and 10^{-1}s^{-1} . The upper bound analysis solutions and the experimental results are comparable. A theoretical dynamic ageing region was found to be in the temperature range of 90 °C to 260 °C, which is in agreement with the experimental observations in the temperature range of 75 °C to 175 °C.

Keywords: severe plastic deformation, metals, aging, deformation, grain refinement

1. INTRODUCTION

In the last two decades polycrystalline metallic ultrafine grained (UFG) [1], nanostructured (NS) materials [2], and amorphous materials [3-5] for light weight and high strength applications have been the subject of intensive study. Severe plastic deformation (SPD) processes, in recent years, have been promising top-down techniques for manufacturing UFG/NS materials by imposing a large amount of strain on a workpiece and for refining grains without any noteworthy change in initial workpiece dimensions [6-8]. Segal [9] first presented the innovative process, naming it 'equal channel angular extrusion/pressing (ECAE/ECAP)', which is now the most common method of SPD.

Extensive investigations into cold or room temperature ECAP of metallic materials have already been undertaken by many research groups. In cold ECAP processing, the plastic deformation theory supposes that flow stress is independent of temperature [9-12], and is dependent on work

hardening and strain rate sensitivity [13-17]. The assumption of strain and temperature independent, strain hardening and strain rate dependent material properties is acceptable for most cases of the cold plastic deformation of metallic materials, but at elevated temperatures the flow stress of metallic materials is affected considerably by both temperature and strain rate [18,19]. Severe plastic deformation behavior during elevated temperature ECAP is relatively rare compared to during room temperature ECAP. Recently, papers on elevated temperature ECAP have been both qualitative and empirical [20-22].

Medium-strength Al alloys based on the Al-Mg-Si system (6xxx series) have many applications as extrusions in the automobile and the aerospace industries [23]. Xu *et al.* [13] found that ECAP is effective in reducing the grain sizes in six different Al-based alloys. Ferrasse *et al.* [24] studied the effect of pre-ECAP heat treatment on the strength of alloys and found that the strength of ECAP processed peak-aged alloy reached 400 MPa at the strain of 4. The effectiveness of strengthening aged Al alloys treated by ECAP may be influenced by the stability of precipitates and by the dislocation accumulation during ECAP [25]. The deformation behavior of Al alloys is generally influenced by the pres-

*Corresponding author: ktaheri@sharif.edu

ence of precipitates; therefore, plastic flow during ECAP may be influenced by the presence and the amount of precipitates [26].

Whereas previous studies have not addressed the effects of temperature and strain rate on the mechanics of ECAP at elevated temperatures, in the present study an upper bound solution is presented to theoretically consider the effects of temperature and strain rate on plastic flow behavior during the ECAP process. In particular, the present analysis is focused on the dynamic ageing phenomenon related to ECAP.

2. MATERIALS AND TESTING

The Al-6082 alloy rod used in this study had the following composition in wt%: 1.3Mg, 0.82Si, 0.5Mn, 0.1Cu, 0.2Fe and balanced Al. It was received in the form of 15 mm diameter rods with T6 heat treatment. The specimens were annealed at 530 °C for 3 hours, and then water quenched to 20°C. Tensile tests were carried out using an Instron 4486 machine to evaluate the mechanical properties related to the dynamic strain ageing treatment. The samples were machined according to the ASTM-E8 Standard. Several different testing conditions were considered as follows: four strain rates of $10^{-4} s^{-1}$, $10^{-3} s^{-1}$, $10^{-2} s^{-1}$, and $10^{-1} s^{-1}$, and temperatures from room temperature up to 400 °C with intervals of 65 °C. Temperature variations during the tensile testing were found not to exceed 2 °C. The force-displacement curves were converted into engineering stress-strain curves for justifying and calculating the material constants for the upper bound analysis method.

For the ECAP processing, samples 14 mm in diameter and 40 mm in length were machined from a rod. The ECAP processing was performed at temperatures from room temperature up to 200 °C using an Amsler pressing machine with a system for measuring load-displacement curves. The die used in this work has circular channels with an angle of 90°. The lubricant used was a suspension of graphite and molybdenum disulphide (MoS₂). All the apparatuses used for measurement were calibrated accurately before testing.

3. UPPER BOUND MODEL

An upper bound analysis predicts a load that is equal to or greater than the exact load required for plastic flow in metal forming. A kinematically admissible velocity field should therefore be defined as one that satisfies both the incompressibility and the velocity boundary conditions. The real velocity field should minimize the following energy J expression described by Altan et al. [27]:

$$J = \frac{2}{\sqrt{3}} \bar{\sigma} \int_V \sqrt{\frac{1}{2} \dot{\epsilon}_{ij} \dot{\epsilon}_{ij}} dV + \int_{S_v} \bar{\tau} |v| ds - \int_{S_t} T_i v_i ds \tag{1}$$

where $\bar{\sigma}$ and $\bar{\tau}$ are the yield stresses in tension and shear, respectively, V is the region where plastic deformation takes place, S_v is the part of the boundary of V where the velocity discontinuity occurs, S_t is the part of the boundary of V where the tractions are given, |v| is the velocity discontinuities given on S_v, and T_i is the tractions given on S_t. In Eq. 1 the material is assumed to be a rigid-plas-

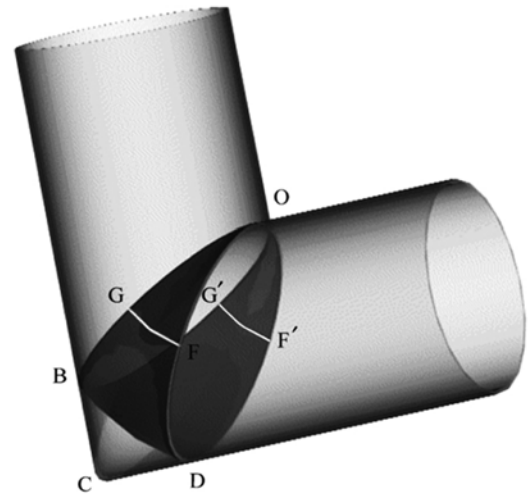
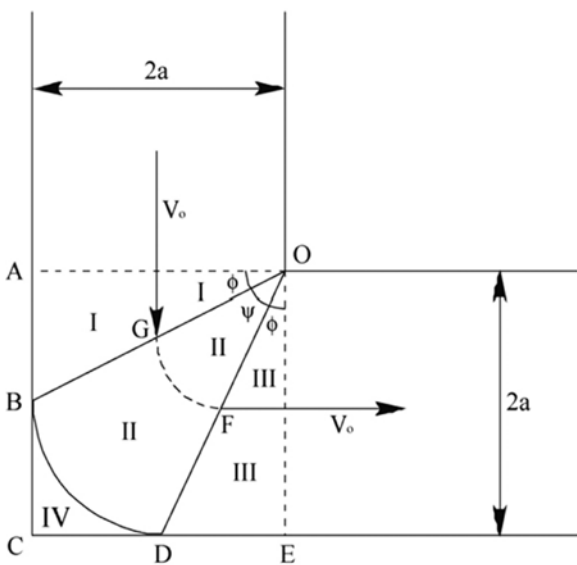


Fig. 1. Two and three dimensional models used in the analysis of ECAP process [28].

tic Von Mises material [27].

The upper bound model for circular cross-section ECAP proposed by Paydar *et al.* is described below. The hypothesized model of the velocity field is shown in Fig. 1. The inlet and outlet shear surfaces are assumed to be flat. It is assumed that under a steady state deformation, a particle enters the shear surface with a uniform linear velocity V_0 , parallel to the vertical channel's axis.

In many prior works flow stress is assumed to be constant throughout the straining [14]. Paydar *et al.* [28] used mean flow stress rather than constant flow stress. Although this method is superior to using constant flow stress, it is still subject to errors. For the present aluminum alloys with strain hardening characteristics, it could be assumed that the true stress-true strain curve obeys the following power relationship:

$$\sigma = K\varepsilon^n \quad (2)$$

The other major effects of strain rate and temperature are theorized to be related to only one parameter known as the velocity-modified temperature (\bar{T}) [29]. That is defined as:

$$\bar{T} = T[1 - \alpha \ln(\dot{\varepsilon}/\dot{\varepsilon}_0)] \quad (3)$$

where T , $\dot{\varepsilon}$ and $\dot{\varepsilon}_0$ are extrusion temperature, effective strain rate and model parameter, respectively, and α is the constant. The value of α was established by trial and error and from the various revised graphs, a value of 0.08 was determined. By plotting the curves of flow stress against \bar{T} for various values of strain, this value of α gave curves of similar shape for various strains.

In high strain-rate forming, the heat generated by the plastic deformation results in thermal softening. If the deformation occurs slowly, most of the generated heat is conducted and/or convected away from the slowly deforming zone and the body remains in an isothermal condition [30]. Before using Eq. 2, some calculations must be performed. First, all temperatures and strain rates must be changed into terms of \bar{T} . The strength coefficient (K) and work hardening exponent n of the Al-6082 specimens were measured by plotting $\log(\sigma)$ versus $\log(\varepsilon)$ [31]. Also the ECAP pressure was calculated by the following Eq. 4 [28]:

$$\frac{P}{\sigma} = \frac{1}{\sqrt{3}}$$

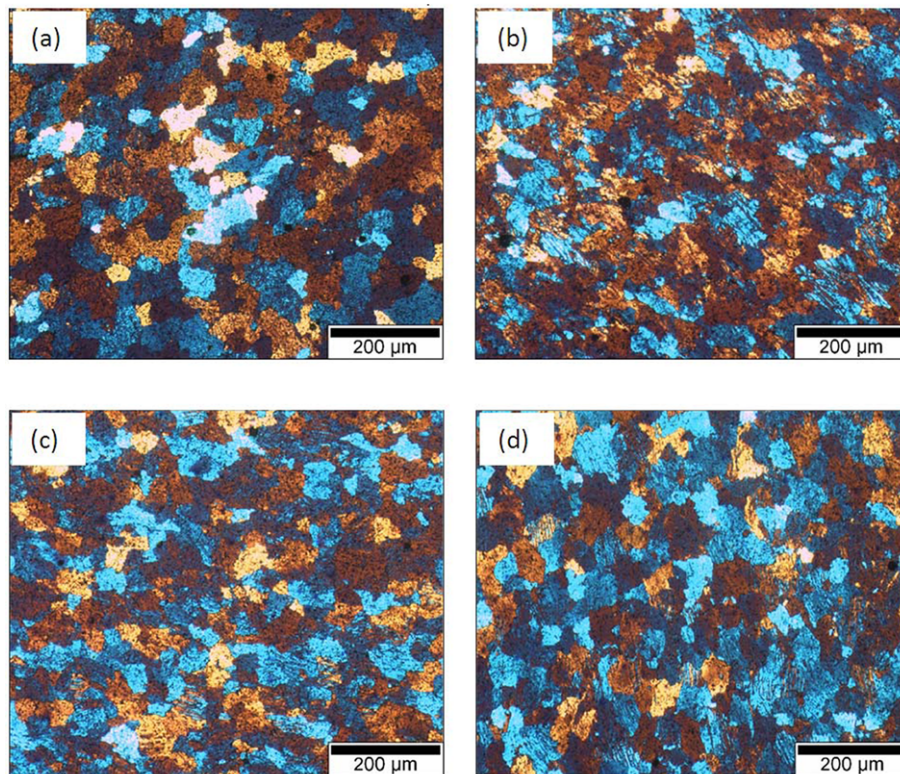


Fig. 2. Polarized-light micrographs of materials (a) as-received (extruded Al6082-T6), and after one pass ECAP at the ram speed of 3.6 mm/min and at (b) 100 °C, (c) 150 °C and (d) 200 °C.

$$\left[\begin{aligned} & \left(\frac{\pi}{2} - 2\phi \right) + 4m \tan \phi + 2 \tan \phi + \left(\frac{2}{\pi} \right) \left(\frac{\pi}{2} - 2\phi \right) \left(\frac{3 \tan^2 \phi}{2} + 1 \right) \cos \phi \\ & + m \left(\frac{2}{\pi} \right) \left(\frac{\pi}{2} - 2\phi \right) \left(\frac{\tan^2 \phi}{2} + 1 \right) \cos \phi + 2m \left(\frac{l}{a} \right) \end{aligned} \right] \quad (4)$$

where P is the ECAP pressure, σ is the flow stress, m is the constant friction factor, l is the length of the specimen and a is the diameter of the die channels.

4. RESULTS AND DISCUSSION

Revealing the grain boundaries of aluminum alloys, especially the 6xxx group, through light microscopy is very difficult due to the high stacking-fault energy of the alloys and the high volume fraction of precipitates in the alloys. In the present study, polarized light microscopy was selected to replace conventional light microscopy. Figure 2 shows polarized optical micrographs of the initial undeformed sample (a) and the ECAP processed samples (b) to (d). The micrographs were all taken from the transverse direction; because when observed in the longitudinal direction, the grains appear to have been severely deformed, and the determination of grain size was not possible. With the microstructure measurement software that was a feature of the microscope, the average grain size of the as-received material was determined to be 103 μm . The average grain sizes of the ECAP processed materials at ram speed of 3.6 mm/min under the processing temperatures of 100 $^{\circ}\text{C}$, 150 $^{\circ}\text{C}$ and 200 $^{\circ}\text{C}$ were 99 μm , 105 μm and 115 μm , respectively. The grain size of material does not change significantly after one pass, but the percentage of equiaxed grains was decreased. Only at a temperature of 200 $^{\circ}\text{C}$ there is some grain growth due to high temperature.

Figures 3 and 4 demonstrate the experimental variations of K and n against the velocity-modified temperature (\bar{T}). The curves of K and n against \bar{T} were approximated by suitable polynomial curve fitting. Thus, for a particular value of \bar{T} , the real values of flow stress pertaining to certain strain, strain rate and temperature can be calculated by Eq. 2. Realistic constitutive modeling of materials of large strains and high strain rates, including temperature effects, is a complex task [30]. The stress value decreases with temperature, hence the work hardening exponent n and the coefficient K decrease as well.

As indicated in Figs. 3 and 4, the values of both K and n increase with temperature in the temperature range of between 90 $^{\circ}\text{C}$ and 260 $^{\circ}\text{C}$. This is a sign of occurring dynamic strain ageing. Also Fig. 5 shows the dependence of strain rate sensitivity on temperature for the present alloy. It is clear

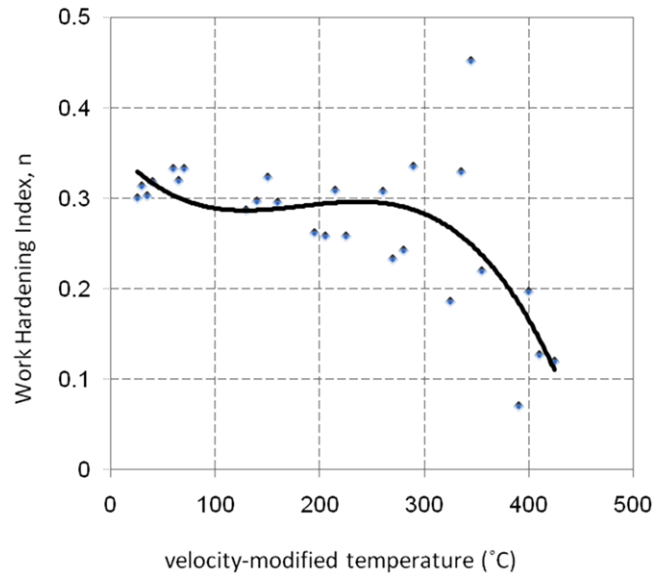


Fig. 3. Variation of work hardening index against velocity-modified temperature.

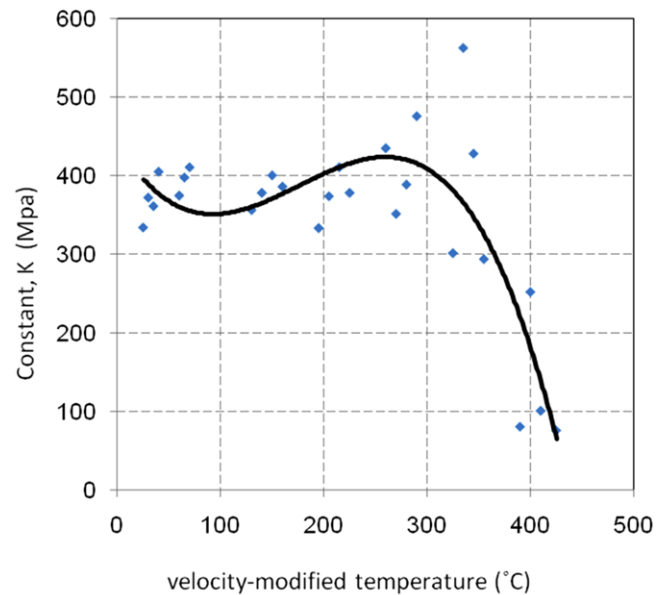


Fig. 4. Variation of coefficient K against velocity-modified temperature.

that the strain rate sensitivity (m) is negative from room temperature up to about 250 $^{\circ}\text{C}$, which is additional evidence of dynamic ageing [32].

The dependence of ECAP pressure (Eq. 4) versus velocity-modified temperature is shown in Fig. 6. Experimental results clearly show three different regions: gradual softening, dynamic ageing and rapid softening. Typical trends of theoretical results for the alloy are shown in Fig. 7. The experimental results are superim-

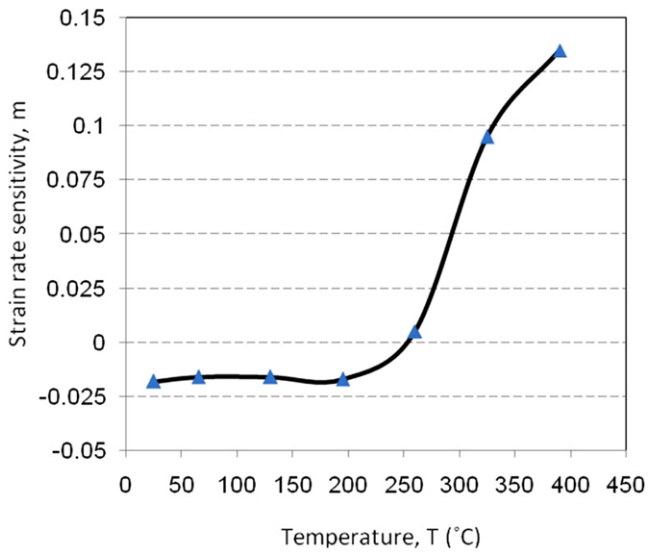


Fig. 5. Variation of strain rate sensitivity against temperature for Al-6082 alloy.

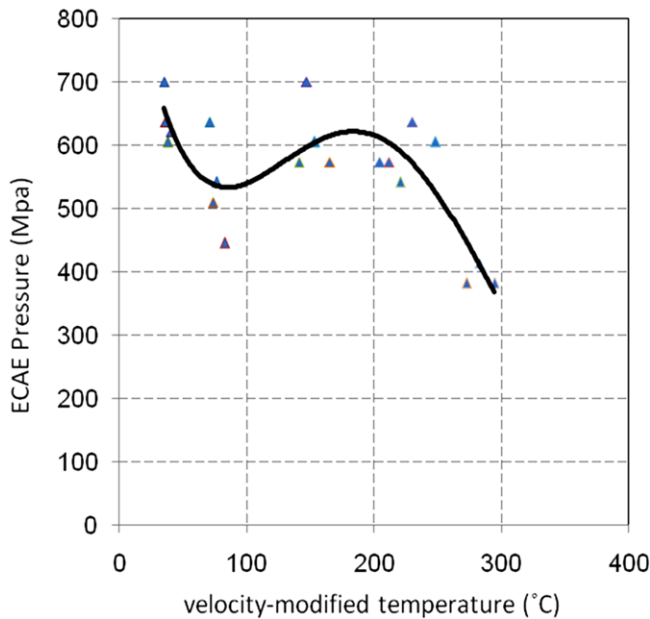


Fig. 6. The pressure of extrusion vs. velocity-modified temperature.

posed onto the theoretical results. It is evident from Figs. 6 and 7 that the predicted curves follow the shape of the experimental curves.

The theoretical responses of the material to temperature are similar to those found experimentally. Although experimental and theoretical results for the strain ageing regions do not match exactly, they are a logically close approximation. However, there are some differences between the uniaxial tension and ECAP which may

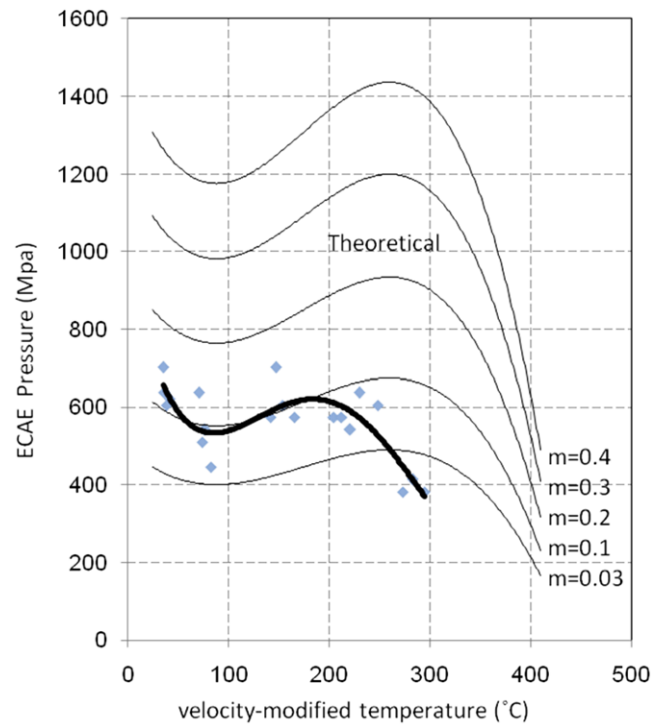


Fig. 7. Comparison of experimental and theoretical results at various temperatures and friction constants.

account for the observed results. ECAP may operate to reduce the strain rate or temperature range related to dynamic strain ageing. Karimi Taheri *et al.* [33] obtained the same results related to dynamic strain ageing during wire drawing of low carbon steel rods. The hydrostatic pressure [32] developed during ECAP acts to increase the density of mobile dislocations. Also in the case of ECAP there is a noteworthy inhomogeneous deformation arising from the redundant strains originated by the shape of the deformation zone. Therefore ECAP produces higher strains than uniaxial tensile testing due to the higher dislocation densities that are developed. Consequently the strain induced during the ECAP process is naturally higher than that produced during conventional tensile testing. On the other hand, the gradual decreasing of the specimen's length causes a decrease of frictional surface area in the entrance channel when the ram moves ahead.

Velocity-modified temperature is dependent mainly on press speed. A change in the press speed will thus cause a change in \bar{T} and therefore in the K and n values, thus taking care of the dynamic ageing phenomenon. At a very low pressing speed, the temperature rise resulting from deformation heating is minor and thus can be ignored [18,34].

From Fig. 7 it can be seen that an increase in the value of

friction factor m does not change the dynamic ageing region. This is because an increase in m causes a temperature rise at the die-specimen interface only if adiabatic conditions are assumed. When the ECAP temperature increases, a good correlation is not found between the experimental and the theoretical results.

In general, an increase in m does not significantly change the \bar{T} value within the deformation zone and thus the values of K and n are not significantly affected, therefore, m does not affect the dynamic ageing region. Referring again to Fig. 7, the differences between ECAP pressures decrease as temperature increases. This is probably because at high temperatures there is a simultaneously decreasing of the values of K and n , which are the material parameters not processing parameters.

In addition to the influence of the previously mentioned factors of the ECAP process, it was determined that due to an increase in temperature at the die-specimen interface there is a breakdown of the lubricant which makes an analysis of this condition more complex.

5. CONCLUSIONS

A theoretical study of the ECAP process at elevated temperatures has been made for a range of strain rates. The trend of the theoretical results obtained from the upper-bound solutions generally follows that of the experimental results for the present alloy. At lower temperatures (25 °C to 175 °C), the theoretical ECAP pressure achieved from the upper bound model was in good agreement with the experimental results. The theoretical ECAP pressure curves have been found to follow the shape of the experimental curves. A dynamic ageing region was theoretically determined to be in the temperature range of 90 °C to 260 °C; this was in good agreement with that observed experimentally, in the temperature range of 75 °C to 175 °C. It can be concluded that the derived upper-bound analysis can be used to predict the equal channel angular extrusion pressure with reasonable accuracy if an accurate value of the friction factor is known for higher temperatures.

ACKNOWLEDGMENTS

M. Vaseghi and A. Karimi Taheri would like to thank the Iran National Science Foundation and the Sharif University of Technology, Tehran, Iran for their financial support. Helpful discussion with Prof. S. I. Hong (Chungnam National University) has improved the quality of the paper. HSK acknowledges the support by a grant from the Center for Advanced Materials Processing (CAMP) of the 21st Century Frontier R&D Program funded by the

Ministry of Knowledge Economy, Republic of Korea.

REFERENCES

1. H. S. Kim and Y. Estrin, *Appl. Physics Lett.* **79**, 4115 (2001).
2. H. S. Kim, C. Suryanarayana, S.-J. Kim, and B. S. Chun, *Powder Metall.* **41**, 217 (1998).
3. S. J. Hong, H. S. Kim, T. S. Kim, W. T. Kim, and B. S. Chun, *Mater. Sci. Eng.* **A271**, 469 (1999).
4. H. S. Kim, *Mater. Sci. Eng.* **A304-306**, 327 (2001).
5. H. Kato, K. Yubuta, D.V. Louzguine, A. Inoue, and H. S. Kim, *Scripta mater.* **51**, 577 (2004).
6. R. Valiev, Y. Estrin, Z. Horita, T. G. Langdon, M. J. Zehetbauer, and Y. T. Zhu, *JOM* **58**, 33 (2006).
7. A. V. Nagasekhar and H. S. Kim, *Met. Mater. Int.* **14**, 565 (2008).
8. Y. H. Jang, S. S. Kim, S. Z. Han, C. Y. Lim, and M. Goto, *Met. Mater. Int.* **14**, 171 (2008).
9. V. M. Segal, *Sc.D. Thesis*, p. 45-112, Ufa State Aviation Technical University (USATU), Minsk, Russia (1974).
10. S. C. Baik, Y. Estrin, H. S. Kim, R. Hellmig, and H. T. Jeong, *Mater. Sci. Forum* **408-412**, 697 (2002).
11. S. C. Baik, Y. Estrin, R. J. Hellmig, H. T. Jeong, H.-G. Brokmeier, and H. S. Kim, *Z. Metallkd.* **94**, 1189 (2003).
12. H. S. Kim, *Mater. Trans.* **42**, 536 (2001).
13. C. Xu, M. Furukawa, Z. Horita, and T. G. Langdon, *Acta mater.* **51**, 6139 (2003).
14. H. S. Kim, M. H. Seo, and S. I. Hong, *J. Mater. Process. Tech.* **130**, 497 (2002).
15. J.-H. Han, H.-J. Chang, K.-K. Jee, and K. H. Oh, *Met. Mater. Int.* **15**, 439 (2009).
16. S. C. Yoon, A. V. Nagasekhar, and H. S. Kim, *Met. Mater. Int.* **15**, 215 (2009).
17. H. S. Kim, W. S. Ryu, M. Janecek, S. C. Baik, and Y. Estrin, *Advanced Eng. Mater.* **7**, 43 (2005).
18. Q. X. Pei, B. H. Hu, C. Lu, and Y. Y. Wang, *Scripta mater.* **49**, 303 (2003).
19. Y. Nishida, T. Ando, M. Nagase, S. Lim, I. Shigematsu, and A. Watazu, *Scripta mater.* **46**, 211 (2002).
20. M. Cai, D. P. Field, and G. W. Lorimer, *Mater. Sci. Eng.* **A373**, 65 (2004).
21. M. Cai, G. W. Lorimer, and D. P. Field, *Mater. Forum* **28**, 406 (2004).
22. M. Cai and G. J. Cheng, *JOM* **59**, 58 (2007).
23. M. Cai, J. D. Robson, and G. W. Lorimer, *Scripta mater.* **57**, 603 (2007).
24. S. Ferrasse, V. M. Segal, K. T. Hartwig, and R. E. Goforth, *J. Mater. Res.* **12**, 1253 (1997).

25. B. S. Moon, H. S. Kim, and S. I. Hong, *Scripta mater.* **46**, 131 (2002).
26. A. S. M. Agha, *J. Mater. Process. Tech.* **209**, 856 (2009).
27. B. S. Altan, G. Purcek, and I. Miskioglu, *J. Mater. Process. Tech.* **168**, 137 (2005).
28. M. H. Paydar, M. Reihanian, R. Ebrahimi, T. A. Dean, and M. M. Moshksar, *J. Mater. Process. Tech.* **198**, 48 (2008).
29. C. W. MacGregor and J. C. Fisher, *J. Appl. Mech.* **13**, A11 (1946).
30. R. Liang and A. S. Khan, *Int. J. Plast.* **15**, 963 (1999).
31. W. F. Hosford and R. M. Caddell, *Metal Forming: Mechanics and Metallurgy*, p. 77-106, Englewood Cliffs (1983).
32. P. G. McCormick, *Acta metal.* **22**, 489 (1974).
33. A. Karimi Taheri, T. M. Maccagno, and J. J. Jonas, *ISIJ Int.* **35**, 1532 (1995).
34. H. S. Kim, *Mater. Sci. Eng. A* **503**, 130 (2008).